НАУЧНО-ТЕХНИЧЕСКИЙ ВЕСТНИК ИНФОРМАЦИОННЫХ ТЕХНОЛОГИЙ, МЕХАНИКИ И ОПТИКИ
ноябрь–декабрь 2025 Том 25 № 6 http://ntv.ifmo.ru/
SCIENTIFIC AND TECHNICAL JOURNAL OF INFORMATION TECHNOLOGIES, MECHANICS AND OPTICS
November–December 2025 Vol. 25 No 6 http://ntv.ifmo.ru/en/
ISSN 2226-1494 (print) ISSN 2500-0373 (online)

НАУЧНО-ТЕХНИЧЕСКИЙ ВЕСТНИК
ИНФОРМАЦИОННЫХ ТЕХНОЛОГИЙ, МЕХАНИКИ И ОПТИКИ

doi: 10.17586/2226-1494-2025-25-6-1208-1219

Aerodynamic analysis of SD7037 airfoil with flex-skin flap at low angles of attack and low Reynolds numbers

Ahmed Tawfeeq Mustafa Ali Abed[1]✉, Azad A. Hussein[2], Saba Hafedh Mahdi[3]

[1,2,3] Aeronautical Engineering Department, College of Engineering, University of Baghdad, Baghdad, 10071, Iraq

[1] a.t.abed@coeng.uobaghdad.edu.iq✉, https://orcid.org/0000-0002-8025-9367
[2] azad.a@coeng.uobaghdad.edu.iq, https://orcid.org/0000-0001-9792-7774
[3] saba.hafedh@coeng.uobaghdad.edu.iq, https://orcid.org/0009-0009-9479-0536

Abstract

This work concentrates on the effect of a flex-skin trailing edge flap on the aerodynamic characteristics of SD7037 airfoil at low Reynolds numbers, in the range of $2 \cdot 10^5$ to $5 \cdot 10^5$ using computational methods. The study used a range of angle of attack (AOA) associated with the take-off phase and different flap angles. The numerical model was set up in Siemens STAR-CCM+ package using the κ-ω shear stress transport turbulence model and the (γ-Reθ) transition model which ensured the approximate solution of Navier-Stokes equations. The verification of the computational solution was done by the comparison with the available experimental data of the plain flap, and it was discovered that the results matched pretty well at lower AoAs. Results indicated that certain sets of AoAs and flap angles can notably achieve the lift over the drag ratio above the baseline conditions, thus improved the performance especially during take-off stage. Besides, some combinations were found to be inefficient, and these were recommended to be discarded. Additionally, the results showed that the flex-skin flap generated higher lift coefficient but also higher drag coefficient at the same range of AoAs as compared to that of the plain flap.

Keywords

UAV, aerodynamics, lift, drag, performance

For citation: Abed A.T.M.A., Hussein A.A., Mahdi S.H. Aerodynamic analysis of SD7037 airfoil with flex-skin flap at low angles of attack and low Reynolds numbers. *Scientific and Technical Journal of Information Technologies, Mechanics and Optics*, 2025, vol. 25, no. 6, pp. 1208–1219. doi: 10.17586/2226-1494-2025-25-6-1208-1219

УДК 533.6

Аэродинамический анализ профиля SD7037 с гибким закрылком при малых углах атаки и малых числах Рейнольдса

Ахмед Тауфик Мустафа Али Абед[1]✉, Азад А. Хусейн[2], Саба Хафед Махди[3]

[1,2,3] Отделение авиационной техники Инженерного колледжа, Багдадский университет, Багдад, 10071, Ирак

[1] a.t.abed@coeng.uobaghdad.edu.iq✉, https://orcid.org/0000-0002-8025-9367
[2] azad.a@coeng.uobaghdad.edu.iq, https://orcid.org/0000-0001-9792-7774
[3] saba.hafedh@coeng.uobaghdad.edu.iq, https://orcid.org/0009-0009-9479-0536

Аннотация

С использованием вычислительных методов изучено влияние закрылка беспилотного летательного аппарата с гибкой обшивкой на аэродинамические характеристики профиля SD7037 при низких числах Рейнольдса в диапазоне от $2 \cdot 10^5$ до $5 \cdot 10^5$. Исследование проводилось в диапазоне углов атаки (Angles of Attacks, AoAs), связанных с фазой взлета и различными углами закрылка беспилотного летательного аппарата. Численная модель реализована в пакете Siemens STAR-CCM+ с использованием модели турбулентности переноса касательных напряжений κ-ω и модели перехода γ-Reθ, которая обеспечивает приближенное решение уравнений Навье–Стокса. Проверка вычислительного решения выполнена путем сравнения с имеющимися экспериментальными данными, полученными для плоского закрылка. Обнаружено, что результаты довольно хорошо совпадают при более низких AoAs. Показано, что определенные наборы AoAs и углов закрылка могут заметно обеспечить

подъемную силу с аэродинамическим качеством выше базовых условий, тем самым улучшая характеристики, особенно на этапе взлета. Установлено, что некоторые комбинации параметров оказались неэффективными, и от них было рекомендовано отказаться. Обнаружено, что гибкая обшивка закрылка обеспечивает более высокий коэффициент подъемной силы, но также и более высокий коэффициент лобового сопротивления при том же диапазоне углов атаки по сравнению с обычным закрылком беспилотного летательного аппарата.

Ключевые слова

БПЛА, аэродинамика, подъемная сила, сопротивление, производительность, беспилотный летательный аппарат

Ссылка для цитирования: Абед А.Т.М.А., Хусейн А.А., Махди С.Х. Аэродинамический анализ профиля SD7037 с гибким закрылком при малых углах атаки и малых числах Рейнольдса // Научно-технический вестник информационных технологий, механики и оптики. 2025. Т. 25, № 6. С. 1208–1219 (на англ. яз.). doi: 10.17586/2226-1494-2025-25-6-1208-1219

Introduction

Aircraft lift can be boosted by the use of flaps which also affects stall speeds, take-off, and landing distances by lowering these characteristics. These effects are utilized in Unmanned Aerial Vehicles (UAVs) to improve the lift, but with increased drag. The UAV flight stability is also enhanced. At specific situations the efficiency of the airfoil is improved, which in return improves UAVs range. For these positive outcomes various flap types have been formed over the years to get definite aerodynamic characteristics [1, 2]. Flex-skin flaps are very simple and can be easily fabricated with very simple tools and techniques at truncated cost. Comparing to other types of flaps, this minimalism comes with limited reliability that solely depends on the type of the material used to form the skin of the airfoil and the flap, as presented by Ooda [3]. Therefore, studying airfoils with flaps, including flex-skin type, could provide valuable insights for a broad range of UAV engineers, hobbyist, and makers [4].

Literature Review

Due to its obvious importance many studies were carried for various types of flaps on different airfoil sections such as the work done by Frolov and Wenming [5] who analyzed the effect of plain flap on airfoil lift by using computational methods. The complex variable function theory was used to analyze the proposed model accompanied with conformal mapping and the discrete vortex method. The study showed linear relation between the increase of lift coefficient *cl* and the increase of the plain flap angle.

While Todorov [6] analyzed numerically a single slotted flap airfoil NACA-23012, the study included a numerical analysis of aerodynamic coefficient at Reynolds number of $3 \cdot 10^6$ and simulated the forces on the flap using computational fluid dynamics utilized by ANSYS Fluent code. The proposed technique uses a turbulent model with Spalart-Allmaras method. Also, the airfoil has 1 m chord with an additional 0.32 m chord for the slotted flap. The study found out that the slotted flap generated a greater lift coefficient *cl* than that of the (NACA-23012) profile, with less drag coefficient *cl* for the flap model.

Srivastava [7] modeled and analyzed airfoil NACA-2412 with flap to generate high-lift. The 3D model simulated using Reynolds number 1.4 million (velocity 20.42 m/s). The dimensions of the model were 1 m and 0.332 m for the chord and flap, respectively. The study showed that the maximum lift generated at 10° flap angle.

The flap deflection on NACA-2412 airfoil was simulated numerically by Dutta et al. [8]. The flow regime selected to be subsonic. Also, for each angle of attack (AoA) from the set (0°, 4°, 8°, and 12°) the model used a different flap deflection. The model simulated using ANSYS Fluent with structured mesh-grid and the model dimensions set to be 150 mm and 300 mm for chord length and span, respectively. The end results indicated that with the increasing the AoA, the lift coefficient *cl* enhanced up to a certain degree. As well as, the study simulate the relation between different flap deflection and the flight condition.

Also, the airfoil section NACA-2412 with plain flap was studied using computational techniques by Thejarju et al. [9] using ANSYS Fluent for various flap angles. The study showed that the maximum lift coefficient *cl* observed at 32° flap angle.

Because the calculations of aerodynamic forces are accurate for flows where boundary layer transition may occur, such as in wind turbine and in many other crucial aerospace applications, Michna et al. [10] evaluated the accuracy of the γ-Reθ boundary layer transition method in forecasting the aerodynamics of the DU-91-W2-250 profile at high Reynolds numbers. The study inspects transition onset, boundary layer development, and flow separation by comparing numerical results with experimental measurements. While the model effectively gets key transition phenomena, inconsistencies arise in separation-induced transition and turbulent reattachment regions. The findings indicate that γ-Reθ is suitable for preliminary aerodynamic analysis but requires refinements for high-fidelity simulations.

The aerodynamic effects of fixed wing UAV airfoil SD-7037 were numerically evaluated by Ramanan et al. [11]. The model simulated at low Reynolds number, with dimensions of the model (719 mm, 292 mm, and 120 mm for length, width and total height, respectively). The model simulated using ANSYS Fluent. The result showed that the simulation analysis is satisfying to meet the performance aspects.

The change of the flap angle influences on the performance of airfoil type NACA-4415 is studied in the research carried by Vinod and Joth [12]. The model simulated at Reynolds number $4 \cdot 10^6$ and AoA varied from –10° to 30°, using Xfoil software. Also, the flap angle was (–90°, –45°, +45° and +90°). The analysis showed that during the take-off situation the flap can be useful due to

the generation of sudden lift. The viscosity effects were not considered in this work as the Xfoil software provides limited supported for boundary layer simulation.

The lift and drag forces of airfoil (M21) with plain flapper at diverse AoAs was investigated numerically by Patel et al. [13]. The different flapped designs simulated using ANSYS Fluent. Also, the κ-ω turbulence model used with 2,000,006 Reynolds number as initial boundary conditions. The chord length selected to be 1.0148 m. The mesh/grid generation tested around 395,846 elements. The study showed that the drag and lift increase with the AoA increases. The angle of stall found out to be around 24°. The plain flapper angle that improved the lift found out to be around 10°.

Flaps are also used in wind turbines to reap its benefits, thus, Ma et al. [14], simulated numerically and analyzed the effect of adding flap to airfoil S 809 wind turbine. The flap added to the upper surface of the S 809 airfoil with a cord length of 1 meter and the Reynolds number value of $1 \cdot 10^6$. The 2D model was simulated using ANSYS Fluent with 2D incompressible Reynolds Averaged Navier-Stokes (RANS) equations. The total mesh selected to be around 160,000 cells. The study showed that the added flap improve the aerodynamic performance of the optimal performance found out to be at AoA = 14°, where the drag decreased by 3.98 % and the lift increased by 13.67 %.

Computational and experimentally methods was used to investigate the flap angles on the performance of a home-built wing NACA-23012 in the work of Salam et al. [15]. The tested angles of attack were 0°, 5°, 10°, 15° and 20°, and the flap angles were –15°, 0°, 15°, 30°, and 45°. The chord and the span of the model was taken as 1.6 m and 0.29 m, respectively. The study found out that the maximum drag was at 20° AoA and 45° of flap angle. Whereas, the maximum lift was at 0° AoA and at 15° of flap angle. The model optimal performance was at 15° AoA and 45° of flap angle.

Krishnan et al. [16] conducted a simulation to illustrate the consequences of adding flap at different angles on a wing NACA-6412. The AoA for the model varied from –4° to 16° and Mach number from 0.2 to 0.4. The flap angles used were 10°, 20°, and 30°. The model was simulated using ANSYS ICEM CFD. The aerodynamic analysis showed that the maximum lift occurs at 14° AoA. Also, the drag and the lift increased with increasing the flap angle.

Soman et al. [17] investigated the outcomes of changing the numerical settings on the behavior of the γ-Reθ model in simulating both two dimensional and three dimensional bluff body transitional flows using the Open-FOAM software. The influence of various solver configurations and turbulence models on the accuracy and convergence of the simulations was examined, and it was shown that numerical settings significantly affect the transition prediction, especially in complex flow scenarios involving separation and reattachment. The findings emphasize the need for careful optimization of computational parameters to improve the reliability of transition modeling in practical applications, such as aerodynamic design and fluid-structure interaction analysis.

The well-known NACA-4412 airfoil with a plain flap was evaluated numerically by Xiao et al. [18] as this type of airfoil is widely used in UAVs. The simulated model uses κ-ω Shear Stress Transport (SST) method with 1 m chord length and $6 \cdot 10^6$ Reynolds number and around 4° AoA. The study showed that at a certain AoA with increasing the flap angle, the suction shortfall increases on the lower wing surface.

Parluhutan et al. [19] evaluated numerically the effect of plain flap on the lift of symmetrical airfoils NACA-0015. The model simulated at $4 \cdot 10^6$ Reynolds number with κ-Epsilon turbulent model and different angle of deflection of 15° and 30°, the AoA selected to be from 0° to 25°. The study found out that the lift coefficient *cl* increases due to the presence of the flap.

It is worth to mention that less complex methods, other than those that uses control volume methods applied in Computational Fluid Dynamics (CFD), may be used to analyze aerodynamic characteristics of airfoils with flaps, such as the panel method, both linear and non-linear, utilized by Ali [20, 21], but it lacks the capabilities to calculate viscosity effects. These methods can't be used to calculate airfoil performance for practical applications although it requires much less computational power as compared to control volume methods used in this work.

From the presented literature review it can be seen that neither recent nor previous studies have investigated the use of the SD7037 airfoil with a flex-skin flap, in spite of its potential to improve efficiency and its simple manufacturing methods.

This work is a continuation of a previous study carried by Abed [4]. In this work, there exists the aerodynamic performance of the SD7037 airfoil section with trailing edge flex-skin flap, employing CFD at low AoA and Reynolds numbers within the range of $2 \cdot 10^5$ to $5 \cdot 10^5$. The analysis encompasses a variety of low AoA alongside differing flap angles at take-off phase by solving the flow equations of Navier-Stokes by the application of CFD with utilizing κ-ω SST turbulence method and γ-Reθ transition method available in Siemens STAR-CCM+ package to help in the prediction of the performance of UAV during take-off phase.

Numerical Modeling

For this research, the SD7037 airfoil has been selected, with a 0.23 m as the chord length (c) to be compared with the plain flap data from Abed [4]. A flex-skin flap is added to the trailing edge of the airfoil section at the ($0.79c$) position, thus the flap chord is ($0.21c$) of the total chord. The study is carried at sea level conditions. The value of Reynolds number for the flow is set to be ranging from $2 \cdot 10^5$ to $5 \cdot 10^5$.

These settings were preferred to assess the numerical calculations against the experimental measurements for verification, and also to be compared with CFD results from Abed [4]. It is to be noted that no experimental information is available for such case, thus the verification will be carried based on the general behavior of the numerical results for the flex-skin flap with the data from MS Selig et al. [22] for the plain flap of the same airfoil section. The airfoil profile information were based on those from [22] and shaped using utilities provided by the software package, which are presented in Fig. 1.

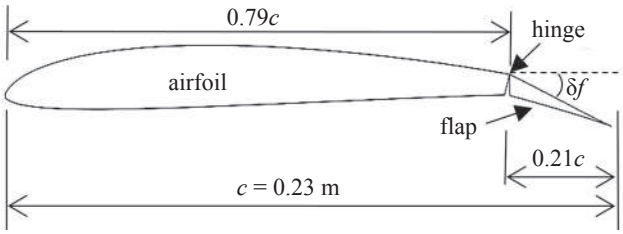

Fig. 1. Drawing of the airfoil and the flex-skin flap with deflection angle δ*f*

For the presented case, it is expected that the flow across the airfoil to be mixed of both laminar and turbulent nature, due to the local Reynolds number could reach and may surpasse the value of $5 \cdot 10^5$, thus become turbulent and encounter a transition phase. Therefore, RANS equations were applied to estimate the viscosity influences. The airfoil has been numerically simulated for steady-state viscous flow conditions at sea level at two dimensions with constant density.

In order to accurately account for the viscosity effects and include the calculations of the transition phenomena, κ-ω with shear stress transport turbulence model presented by Menter, F.R. [23] with γ-Reθ transition method has been selected. The correlations required to formulate this model is based on those typically provided within the model with no calibration, Menter [24].

The computational domain has been chosen to be a square of a large size, 20 m were defined as shown in Fig. 2, this is to eliminate and reduce the effects from the domain boundaries on the airfoil. The inlet has been established to be a velocity inlet, and the outlet at the domain exit was set to a pressure outlet.

Unstructured mesh is preferred to discretize the domain because of its flexibility as presented by Versteeg, H.K. and Malalasekera [25], while a structured mesh was used to model the surface of the airfoil and the flex-skin flap so as to capture the flow nature correctly and in details. The polygonal type of elements has been applied due to their higher quality, accuracy, and stability as compared to the other available types. This type of elements requires more time due its higher requirements of computational power [25].

The boundary layer over the model has been studied, using 60 layers of prism cells near the model solid boundaries. The height of the cell next to the wall calculated to be at $1.2 \cdot 10^{-5}$ m using the method introduced in [25]. The wake of the airfoil was modeled with a length of 20 times of the airfoil chord. Mesh refinement was applied and checked by running a mesh independence study to achieve the accuracy and stability of the solution.

From Fig. 3 below, it can be concluded that the numerical solution will stabilize around 1,563,143 elements, with acceptable accuracy. At higher number of elements the solution become more stable but requires much higher computational power, which will limit the number of cases that can be computed.

Thus, compromise between the level of the accuracy of the solution and the computational power required may be applied. It can be seen from Table 1 below that the difference of the lift coefficient *cl* value between the successive assessments is very small for the last three trials in the mesh independence study, thus the selected mesh yields results with acceptable accuracy and less computational time. Similar technique was used by Abed [4] to increase computational efficiency.

Based on this analysis, the mesh applied in the solution with 1,563,143 elements is presented in Fig. 4 below.

Results and Discussion

As it was mentioned before, the general behavior of the numerical results for the flex-skin flap is compared with that of the experimental measurements from MS Selig, et al. [22] for the plain flap of the same airfoil section in order to verify the correct application of the suggested CFD model.

The behavior of the numerical results show conformity with the experimental information from [22] for the studied cases, as shown in Fig. 5 below, where experimental measurements presented in (Exp) in the figure as solid lines for various flap deflection angles δ*f* are compared to the computational results (CFD) presented in bullets. Thus

Table 1. Change of lift coefficient *cl* among the last trails of the mesh independence study

Number of Elements	Percentage change of lift coefficient *cl* between successive trails, %
1,563,143	0.19
2,635,899	0.11
5,625,178	0.00

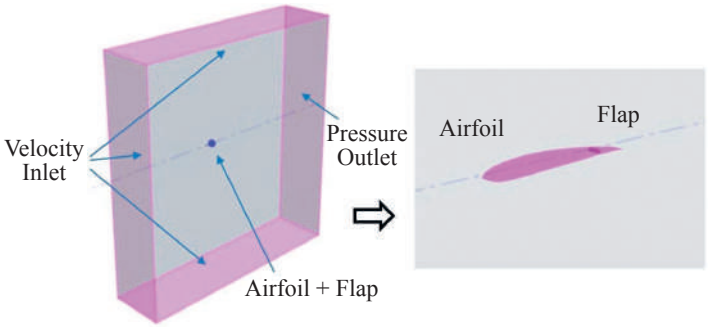

Fig. 2. The computational domain, airfoil with flap

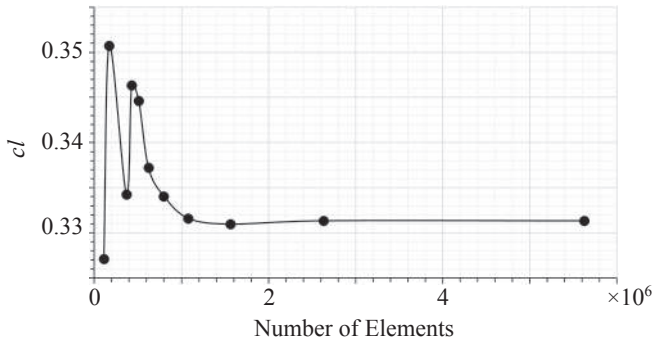

Fig. 3. Mesh Independence Study

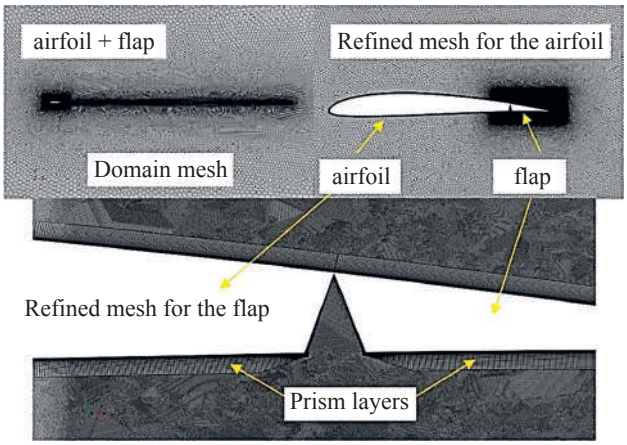

Fig. 4. The applied mesh of the model

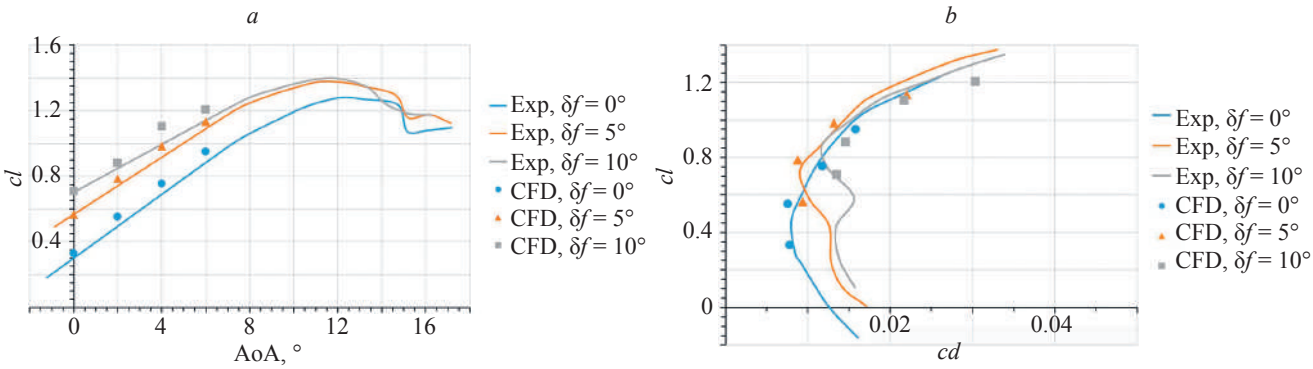

Fig. 5. Validation of CFD results (CFD, bullets) with experimental measurements (Exp, the solid lines) for lift coefficient *cl* (*a*) vs. AoA and drag polar (*b*) vs. drag coefficient *cd* for Reynolds number $3 \cdot 10^5$ for various flap deflection angles in degree

the suggested numerical model may be used to calculate the aerodynamic characteristics for the flex-skin flap on the SD7037 airfoil with acceptable accuracy.

In this work, calculations was carried over the range of AoA from 0° to 6° for a set of various flap deflection angles at 0°, 5°, 10°, 15°, and 20° in the range of Reynolds numbers from $2 \cdot 10^5$ to $5 \cdot 10^5$ with a $0.5 \cdot 10^5$ step, totaling 140 cases. The results are shown and discussed in the following paragraphs.

By the analysis of the computational results shown in Fig. 6, *a–d* below, it can be determined that the value of the lift to drag ratio coefficients (*cl*/*cd*), or the aerodynamic performance of the model, is the highest at AoA 2° at all values of Reynolds numbers, while at AoA 6° is the lowest.

At AoA 2°, δf 10°, Re $3 \cdot 10^5$ further examination of the flow uncovers that near the flap hinge and in the direction of the trailing edge the pressure gradient is unfavorable with many small regions of separated flow as shown in Fig. 7 below. The pressure and velocity contours indicate that drag is much higher in the case of δf 10° as compared to that of δf 5° due to the small regions of flow separations on the upper surface and due to the drop in pressure at the hinge region of the flap on the lower surface.

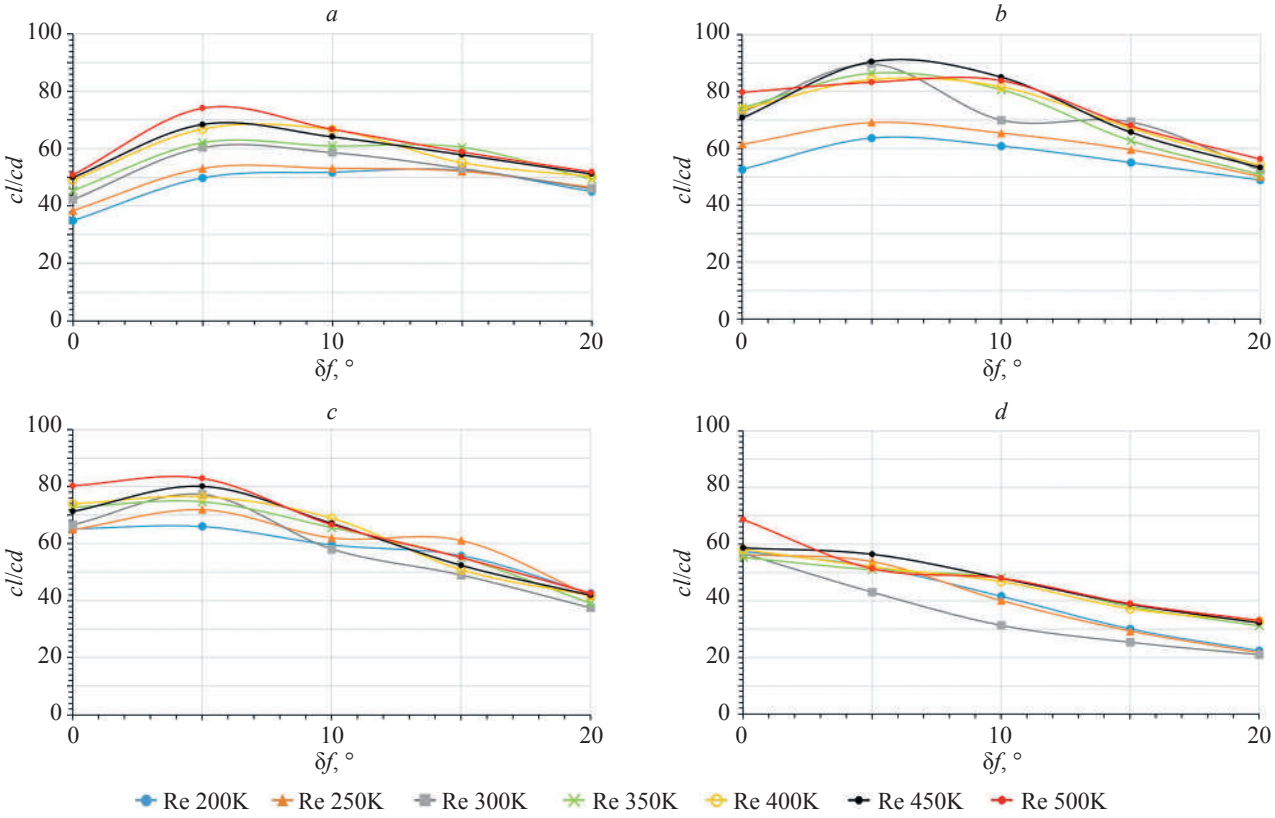

Fig. 6. Lift to drag coefficient ratio *cl*/*cd* of the model at various flap angles for different Reynolds numbers at AoA 0° (*a*), 2° (*b*), 4° (*c*), 6° (*d*)

Fig. 8 shows a closer view of the velocity contours at the flap hinge region which confirms the turbulent nature of the flow near and around the flap.

Fig. 9 demonstrates the moment coefficient (*cm*) as a function of δ*f* for different Reynolds numbers for various AoAs. The moment coefficient *cm* is calculated at the

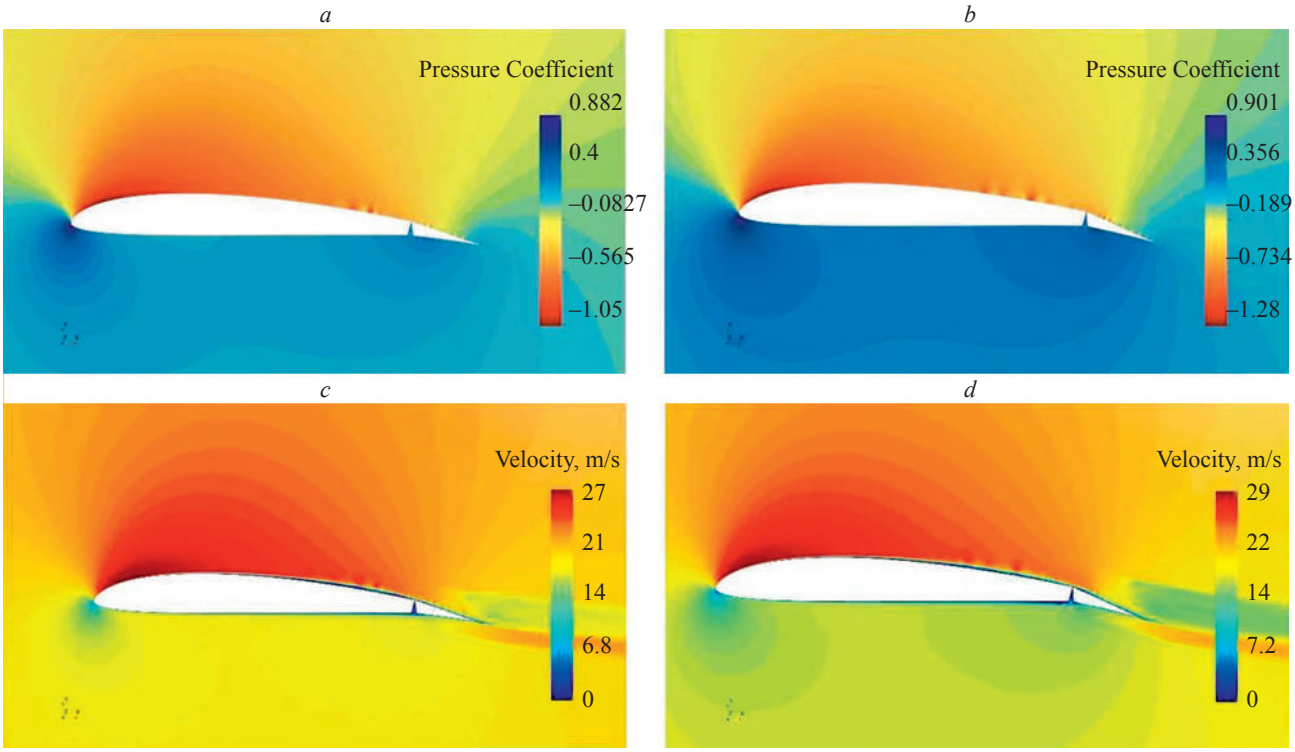

Fig. 7. Pressure and velocity contours at AoA 2°, Re 3·10^5, δ*f* 5° (*a*, *c*), δ*f* 10° (*b*, *d*)

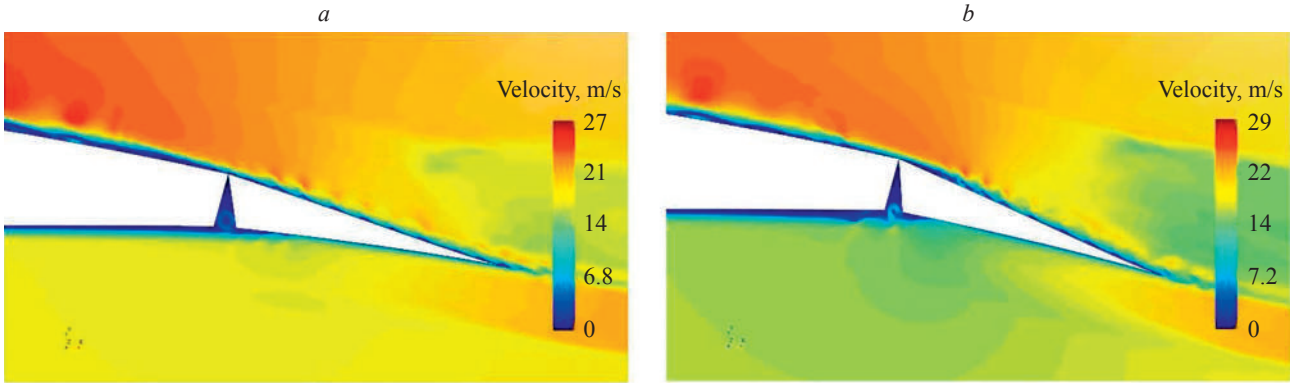

Fig. 8. Velocity contours near flap hinge at AoA 2°, Re 3·10^5, δ*f* 5° (*a*), δ*f* 10° (*b*)

airfoil leading edge with its negative values indicates a counterclockwise direction, or the pitch down moment coefficient *cm*. It can be concluded that as the AoA increases the pitching moment increases as well. This is due to the increase in the forces over the top surface of the model, which means that during take-off a higher δ*f* causes the airfoil to pitch down to counterbalance the moment. It is to be taken into considerations that Reynolds number has a limited effect on the moment coefficient *cm*, except at AoA 6°, δ*f* 20°, as shown in Fig. 9, *d*.

A comparison of the aerodynamic characteristics has been carried between the model with the flex-skin flap and that with the plain flap presented by Abed [4] showed that at Reynolds number of Re 3·10^5 for the lift coefficient *cl* for different AoA at various flap deflection angles is practically the same as can be seen in Fig. 10. This is true except for the situation when the AoA is at 4° and 6° at flap deflection angle of 10°. In those cases the lift for the plain flap model drops noticeably as compared to that of the flex-skin flap. The flex-skin flap retained a more steady

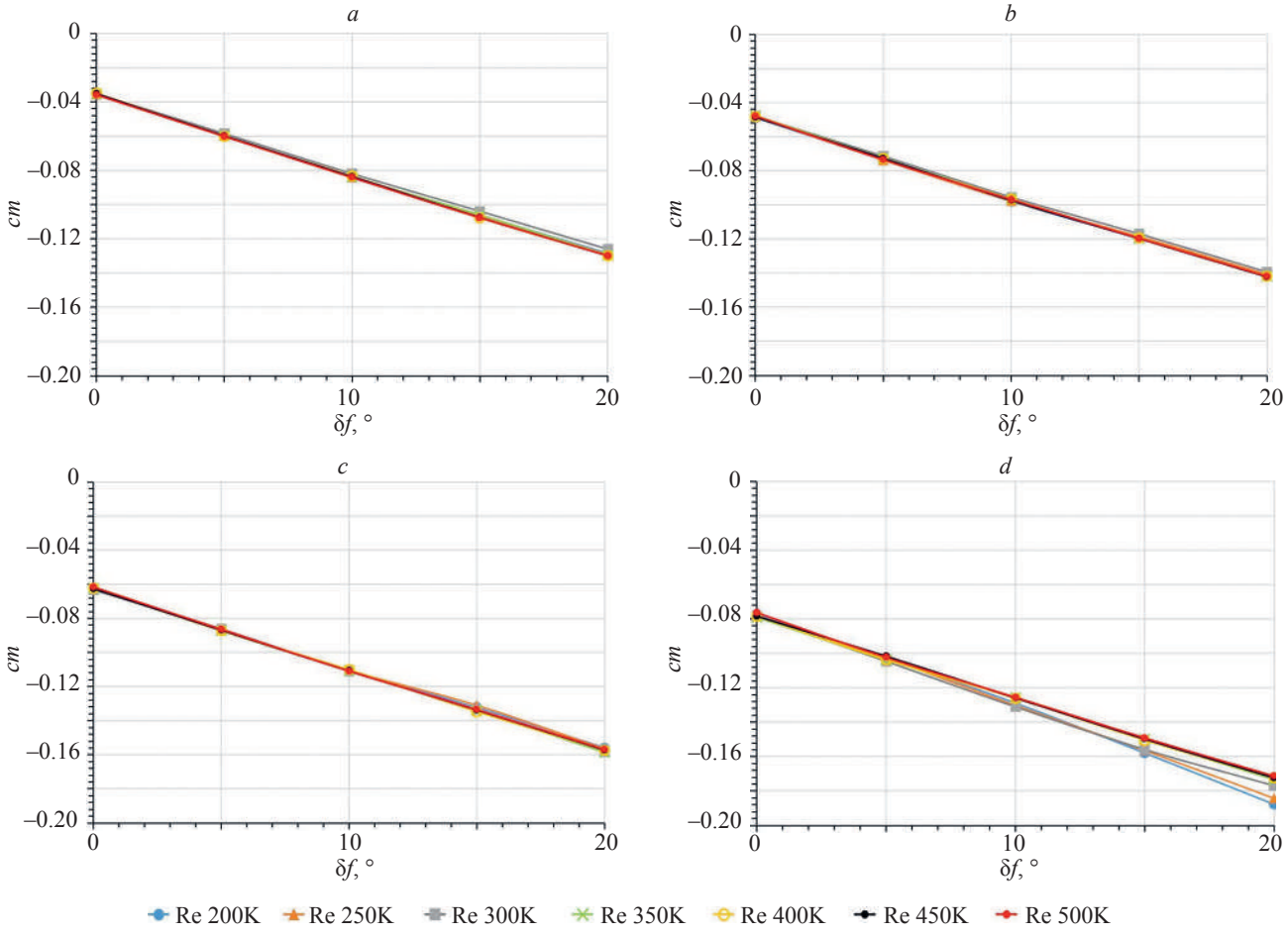

Fig. 9. Moment coefficient *cm* of the model vs. various flap angles for different Reynolds numbers at AoA: 0° (*a*), 2° (*b*), 4° (*c*), 6° (*d*)

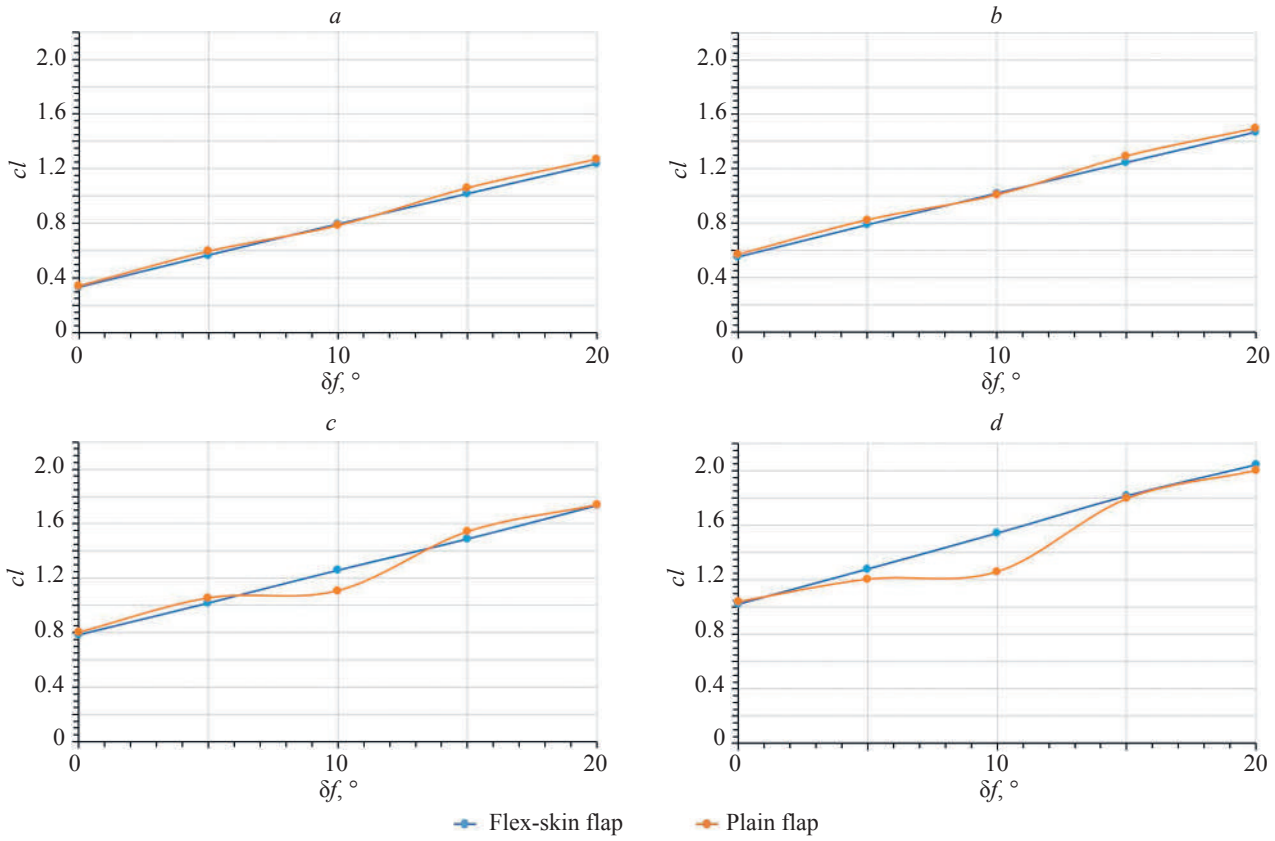

Fig. 10. Lift coefficient *cl* comparison between the flex-skin and the plain flap at Re $3 \cdot 10^5$ for various flap deflection angles at AoA: 0° (*a*), 2° (*b*), 4° (*c*), 6° (*d*)

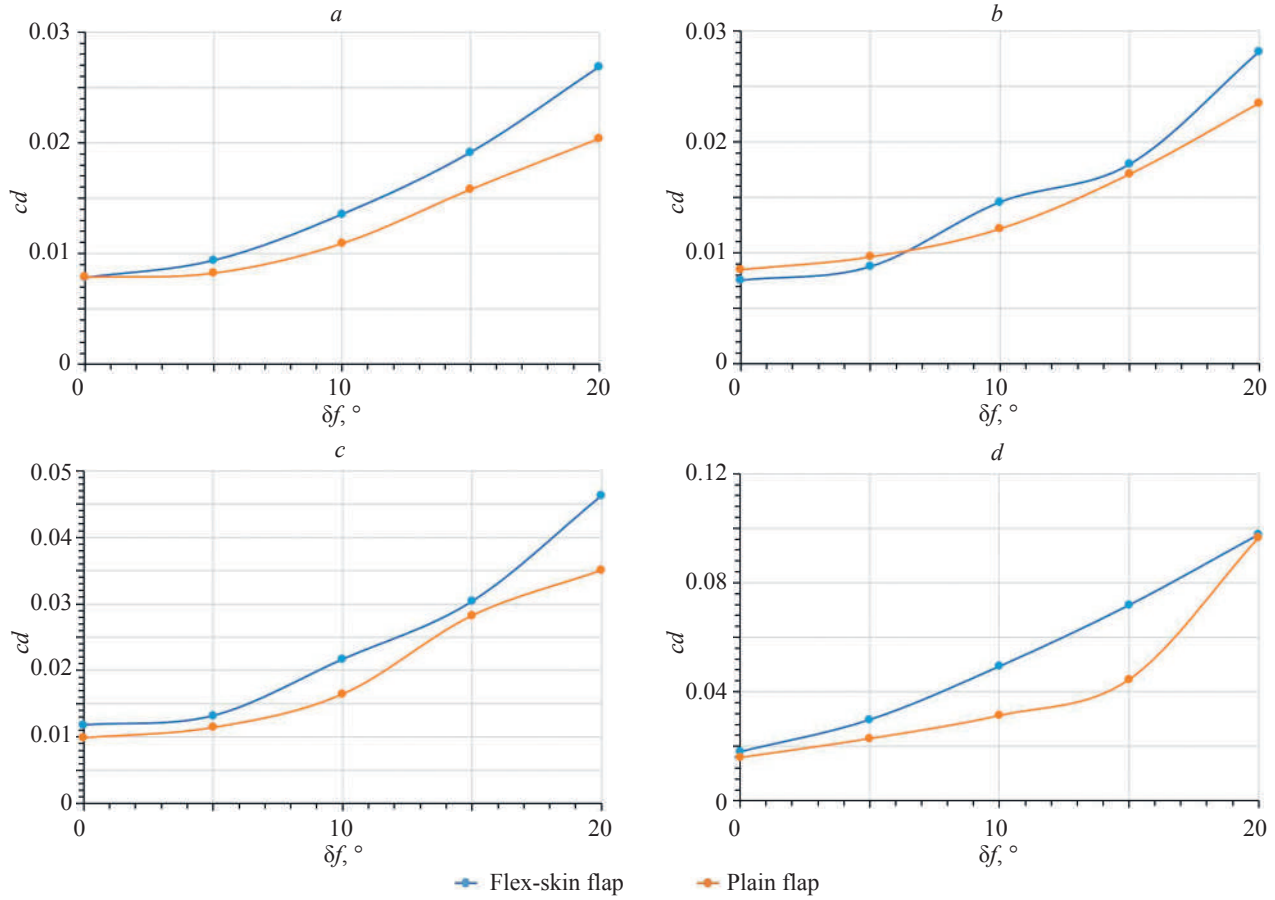

Fig. 11. Drag coefficient *cd* comparison between the flex-skin and the plain flap at Re $3 \cdot 10^5$ for various flap deflection angles at AoA: 0° (*a*), 2° (*b*), 4° (*c*), 6° (*d*)

flow and enhanced pressure gradient over the upper surface due to the continuous surface with no abrupt changes in the geometry.

The flex-skin flap model showed higher drag coefficient *cd* than that of the plain flap as can be concluded from Fig. 11 for the same conditions and cases. This is because of the unsmooth change in the flow route on the bottom surface of the model with flex-skin flap at the hinge point between the wing and the flap. This sudden change of the direction of the flow as it passes the hinge area produced losses of energy resulting in the increase of the drag.

Analysis of the value of the lift to drag of the model presented in the current work as compared to that of the model with the plain flap from Abed [4] is shown in Fig. 12 in similar conditions. It can be deuced that the flex-skin flap offers higher performance at AoAs 0° and 2° while it provides less performance at AoA 4° and 6° with the highest performance recorded at AoA 2° for the model with the plain flap. This is because of the higher drag produced by the application of the flex-skin flap.

The moment coefficient *cm* of the model with the flex-skin flap at Reynolds number of $3 \cdot 10^5$ is compared to that

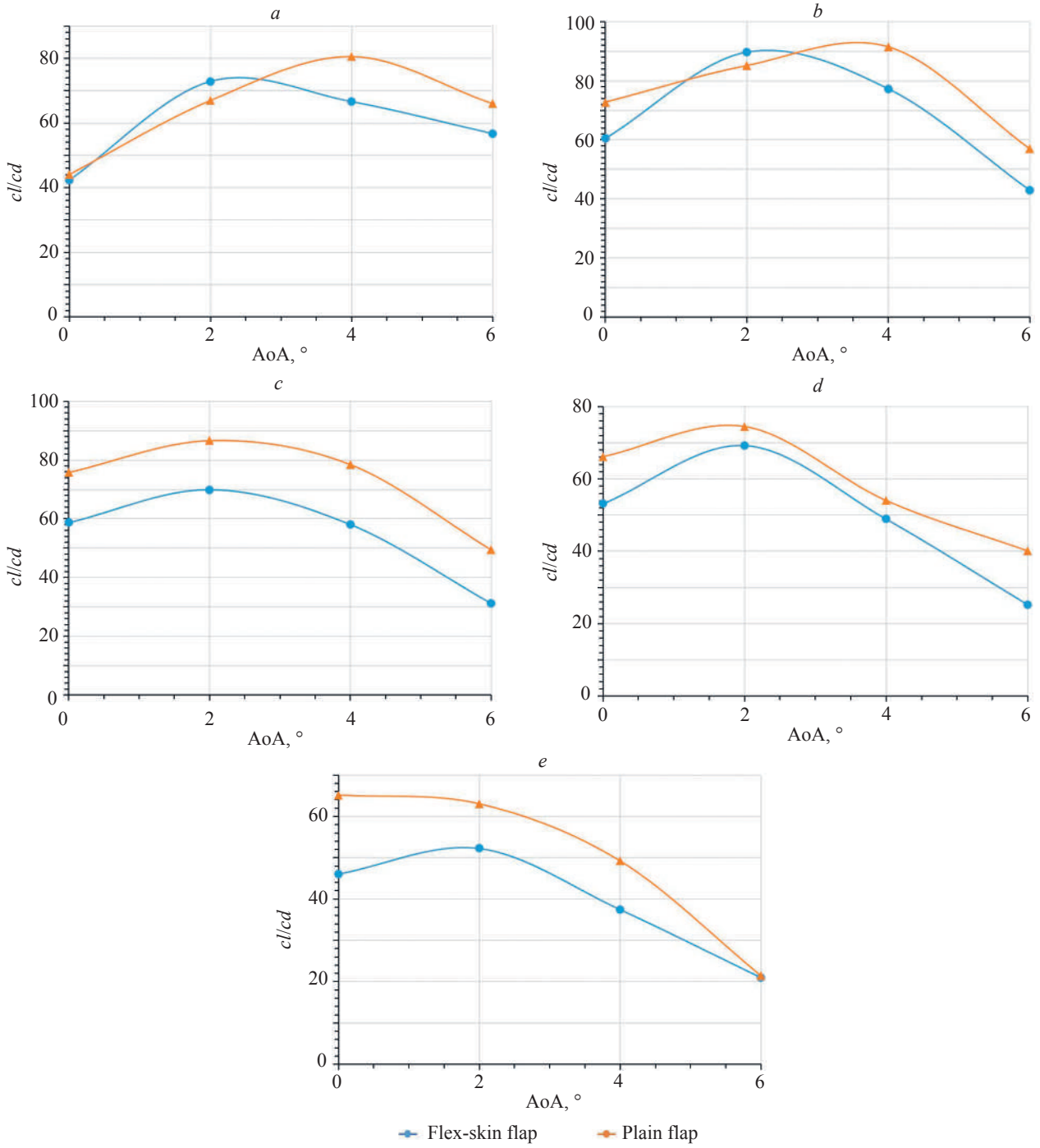

Fig. 12. Lift to drag ratio *cl*/*cd* comparison between the flex-skin and the plain flap at Re $3 \cdot 10^5$ for various angles of attack at δ*f*: 0° (*a*), 5° (*b*), 10° (*c*), 15° (*d*), 20° (*e*)

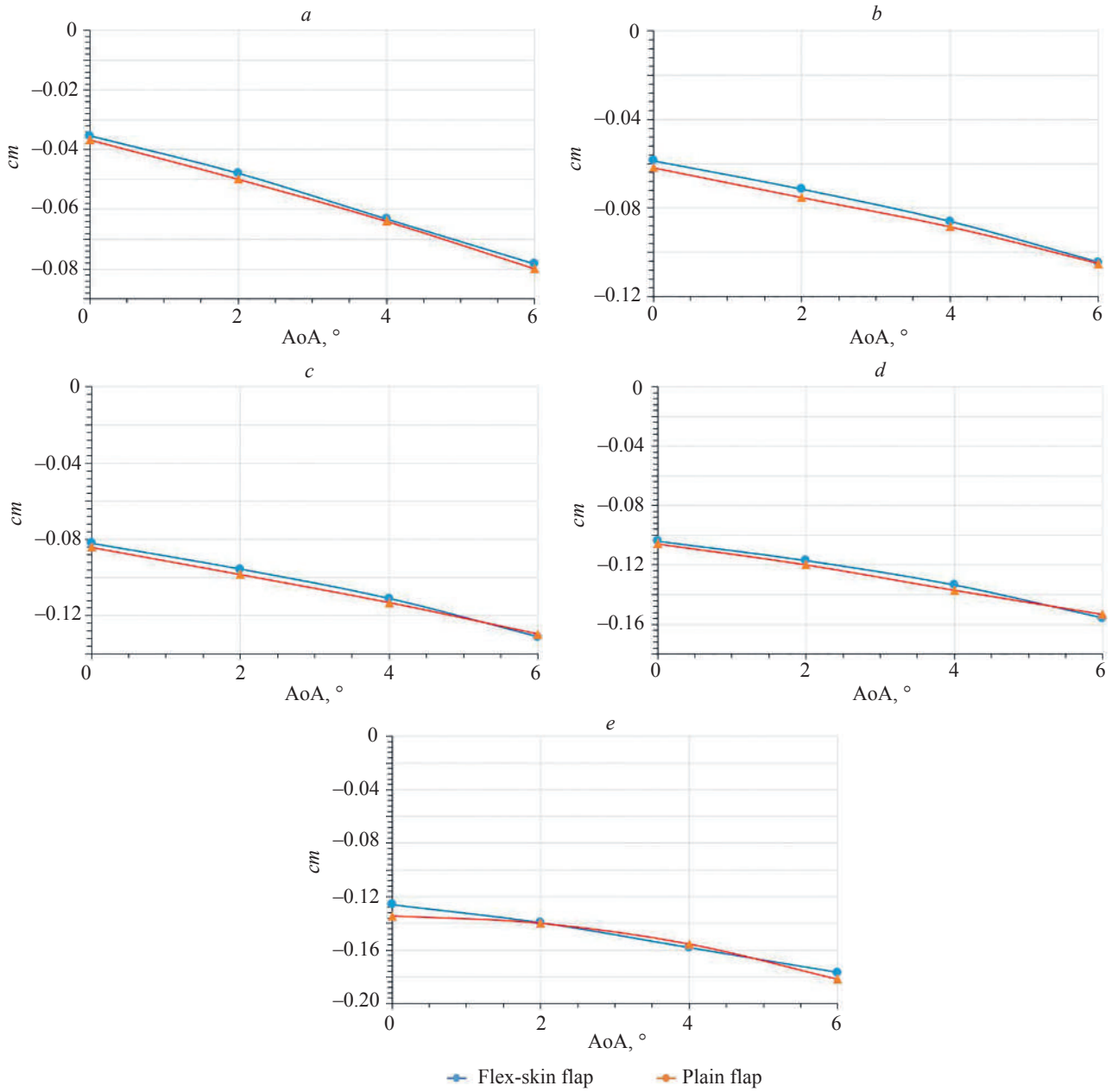

Fig. 13. Moment coefficient *cm* comparison between the flex-skin and the plain flap at Re $3 \cdot 10^5$ for various angles of attack at AoA 0° (*a*), 5° (*b*), 10° (*c*), 15° (*d*), 20° (*e*)

of the plain flap results from Abed [4] which showed that there are insignificant differences, as can be seen in Fig. 13 below.

Conclusion

This research investigates the aerodynamic behavior of an airfoil with SD7037 profile and flex-skin flap at the trailing edge during take-off phase with small Angles of Attack (AoAs) and Reynolds numbers within the range of $2 \cdot 10^5$ to $5 \cdot 10^5$ by the application of Computational Fluid Dynamics (CFD) simulation through the use of Siemens STAR-CCM+ software package.

The research showed that using the κ-ω SST model together with the γ-Reθ transition method is suitable for capturing the complex flow behavior around the SD7037 airfoil with a flex-skin flap at small angles of attack, since it can represent the mixed laminar-turbulent characteristics with acceptable accuracy. The numerical results showed that the best aerodynamic performance, in terms of lift-to-drag ratio, was obtained at a Reynolds number of $4.5 \cdot 10^5$, AoA 2°, and flap deflection angle of 5°. In fact, for the different Reynolds numbers considered, the maximum lift-to-drag ratio consistently appeared at AoA = 2° and $\delta f = 5°$, whereas the lowest lift-to-drag ratio occurred at AoA = 6° for the various flap deflection angles examined. The analysis also indicated that the flex-skin flap can provide a higher lift coefficient *cl* than the plain flap, but this improvement is accompanied by an increase in drag, which ultimately reduces the overall aerodynamic efficiency, even though the pitching-moment coefficient remains comparable.

To further enhance the reliability of the numerical predictions, additional work on the correlations and parameter settings within the γ-Reθ transition model is recommended, particularly with respect to identifying the minimum number of mesh elements needed to maintain solution stability and accuracy. Finally, an experimental investigation is advised to validate and complement the CFD findings presented in this research.

References

1. Anderson J.D. *Introduction to Flight.* McGraw Hill, 2015, 928 p.
2. Sadraey M.H. *Design of Unmanned Aerial Systems*. John Wiley & Sons Ltd., 2020, 637 p.
3. Ooda I.J. Numerical investigation of aerodynamic characteristics of supercritical RAE2822 airfoil with gurney flap. *Journal of Engineering*, 2022, vol. 28, no. 6, pp. 1–14. https://doi.org/10.31026/j.eng.2022.06.01
4. Abed A.T.M.A. Computational analysis of SD7037 airfoil with plain flap. *Archive of Mechanical Engineering*, 2024, vol. 71, no. 4, pp. 561–580. https://doi.org/10.24425/ame.2024.151337
5. Frolov V.A., Dong W.M. Lift investigation of airfoil with flaps. *Applied Mechanics and Materials*, 2014, vol. 627, pp. 89–92. https://doi.org/10.4028/www.scientific.net/AMM.627.89
6. Todorov M.D. Aerodynamic characteristics of airfoil with single slotted flap for light airplane wing. *Proc. of the International Conference of Scientific Paper AFASES*, 2015, pp. 509–515.
7. Srivastava M.S., Aditya C.V.N. Analysis on NACA 2412 airfoil for UAV based on high-lift devices. *International Journal of Engineering Applied Sciences and Technology*, 2016, vol. 1, no. 6, pp. 13–16.
8. Pracheta D., Anup A., Shahriar A., Saifur R.B. Computational study on effect of flap deflection on NACA 2412 airfoil in subsonic flow. *Applied Mechanics and Materials*, 2016, vol. 829, pp. 9–14. https://doi.org/10.4028/www.scientific.net/AMM.829.9
9. Thejaraju R., Dana J., Niveditha V.R., Vishal S., Sumanthran A. A study of airfoil flap deflection angle using CFD simulation techniques. *International Journal of Mechanical and Production Engineering Research and Development (IJMPERD)*, 2019, vol. 9, special issue, pp. 125–132.
10. Michna J., Rogowski K., Bangga G., Hansen M.O.L. Accuracy of the Gamma Re-theta transition model for simulating the DU-91-W2-250 airfoil at high reynolds numbers. *Energies*, 2021, vol. 14, no. 24, pp. 8224. https://doi.org/10.3390/en14248224
11. Ramanan G., Radha Krishnan P., Ranjan H.M. An aerodynamic performance study and analysis of SD7037 fixed wing UAV airfoil. *Materials Today: Proceedings*, 2021, vol. 47, pp. 2547–2552. https://doi.org/10.1016/j.matpr.2021.05.051
12. Abhishek Vinod G., Jothi T.J.S. Effect of flap deflection angle on flow characteristics of aerofoil. *IOP Conference Series: Materials Science and Engineering*, 2021, vol. 1189, no. 1, pp. 012039. https://doi.org/10.1088/1757-899X/1189/1/012039
13. Patel V., Rathod V., Patel C. Numerical investigation of M21 aerofoil and effect of plain flapper at various angle of attack. *Journal of Physics: Conference Series*, 2021, vol. 2070, pp. 012153. https://doi.org/10.1088/1742-6596/2070/1/012153
14. Ma Q., Wang J., Zhang Y., Liu X. Parametric research and aerodynamic performance analysis of wind turbine airfoil with added flap. *AIP Advances*, 2022, vol. 12, no. 10, pp. 105010. https://doi.org/10.1063/5.0109713
15. Salam N., Tarakka R., Jalaluddin, Iriansyah D., Ihsan M. The effects of flap angles on the aerodynamic performances of a homebuilt aircraft wing model. *International Journal of Mechanical Engineering and Robotics Research*, 2022, vol. 11, no. 12, pp. 908–914. https://doi.org/10.18178/ijmerr.11.12.908-914
16. Radha Krishnan P., Mukesh R., Hasan I., Booma Devi P., Alebachew W.A. Comparative study and aerodynamic analysis of rectangular wing using high-lift systems. *International Journal of Aerospace Engineering*, 2023, vol. 2023, pp. 5813557. https://doi.org/10.1155/2023/5813557
17. Soman S., Melvin A., Variya D., Murallidharan J.S. Impact of numerical settings on simulation performance of the Gamma-Re-Theta model for 2D and 3D bluff body transitional flow cases using OpenFOAM. *Lecture Notes in Mechanical Engineering*, 2023, pp. 31–36. https://doi.org/10.1007/978-981-19-6970-6_6
18. Xiao Y., Wang F., Sun P. Numerical simulation of two-dimensional plain flap ground effect based on NACA4412 airfoil. *Journal of Physics: Conference Series*, 2024, vol. 2756, no. 1, pp. 012049. https://doi.org/10.1088/1742-6596/2756/1/012049

Литература

1. Anderson J.D. Introduction to Flight. McGraw Hill, 2015. 928 p.
2. Sadraey M.H. Design of Unmanned Aerial Systems. John Wiley & Sons Ltd., 2020. 637 p.
3. Ooda I.J. Numerical investigation of aerodynamic characteristics of supercritical RAE2822 airfoil with gurney flap // Journal of Engineering. 2022. V. 28. N 6. P. 1–14. https://doi.org/10.31026/j.eng.2022.06.01
4. Abed A.T.M.A. Computational analysis of SD7037 airfoil with plain flap // Archive of Mechanical Engineering. 2024. V. 71. N 4. P. 561–580. https://doi.org/10.24425/ame.2024.151337
5. Frolov V.A., Dong W.M. Lift investigation of airfoil with flaps // Applied Mechanics and Materials. 2014. V. 627. P. 89–92. https://doi.org/10.4028/www.scientific.net/AMM.627.89
6. Todorov M.D. Aerodynamic characteristics of airfoil with single slotted flap for light airplane wing // Proc. of the International Conference of Scientific Paper AFASES. 2015. P. 509–515.
7. Srivastava M.S., Aditya C.V.N. Analysis on NACA 2412 airfoil for UAV based on high-lift devices // International Journal of Engineering Applied Sciences and Technology. 2016. V. 1. N 6. P. 13–16.
8. Pracheta D., Anup A., Shahriar A., Saifur R.B. Computational study on effect of flap deflection on NACA 2412 airfoil in subsonic flow // Applied Mechanics and Materials. 2016. V. 829. P. 9–14. https://doi.org/10.4028/www.scientific.net/AMM.829.9
9. Thejaraju R., Dana J., Niveditha V.R., Vishal S., Sumanthran A. A study of airfoil flap deflection angle using CFD simulation techniques // International Journal of Mechanical and Production Engineering Research and Development (IJMPERD). 2019. V. 9. Special Issue. P. 125–132.
10. Michna J., Rogowski K., Bangga G., Hansen M.O.L. Accuracy of the Gamma Re-theta transition model for simulating the DU-91-W2-250 airfoil at high reynolds numbers // Energies. 2021. V. 14. N 24. P. 8224. https://doi.org/10.3390/en14248224
11. Ramanan G., Radha Krishnan P., Ranjan H.M. An aerodynamic performance study and analysis of SD7037 fixed wing UAV airfoil // Materials Today: Proceedings. 2021. V. 47. P. 2547–2552. https://doi.org/10.1016/j.matpr.2021.05.051
12. Abhishek Vinod G., Jothi T.J.S. Effect of flap deflection angle on flow characteristics of aerofoil // IOP Conference Series: Materials Science and Engineering. 2021. V. 1189. P. 012039. https://doi.org/10.1088/1757-899X/1189/1/012039
13. Patel V., Rathod V., Patel C. Numerical investigation of M21 aerofoil and effect of plain flapper at various angle of attack // Journal of Physics: Conference Series. 2021. V. 2070. P. 012153. https://doi.org/10.1088/1742-6596/2070/1/012153
14. Ma Q., Wang J., Zhang Y., Liu X. Parametric research and aerodynamic performance analysis of wind turbine airfoil with added flap // AIP Advances. 2022. V. 12. N 10. P. 105010. https://doi.org/10.1063/5.0109713
15. Salam N., Tarakka R., Jalaluddin, Iriansyah D., Ihsan M. The effects of flap angles on the aerodynamic performances of a homebuilt aircraft wing model // International Journal of Mechanical Engineering and Robotics Research. 2022. V. 11. N 12. P. 908–914. https://doi.org/10.18178/ijmerr.11.12.908-914
16. Radha Krishnan P., Mukesh R., Hasan I., Booma Devi P., Alebachew W.A. Comparative study and aerodynamic analysis of rectangular wing using high-lift systems // International Journal of Aerospace Engineering. 2023. V. 2023. P. 5813557. https://doi.org/10.1155/2023/5813557
17. Soman S., Melvin A., Variya D., Murallidharan J.S. Impact of numerical settings on simulation performance of the Gamma-Re-Theta model for 2D and 3D bluff body transitional flow cases using OpenFOAM // Lecture Notes in Mechanical Engineering. 2023. P. 31–36. https://doi.org/10.1007/978-981-19-6970-6_6
18. Xiao Y., Wang F., Sun P. Numerical simulation of two-dimensional plain flap ground effect based on NACA4412 airfoil // Journal of Physics: Conference Series. 2024. V. 2756. N 1. P. 012049. https://doi.org/10.1088/1742-6596/2756/1/012049

19. Parluhutan Y.M., Fahrudin F., Rhakasywi D. Investigating the impact of plain flap as lift enhancement on symmetrical airfoils. *International Journal of Marine Engineering Innovation and Research*, 2024, vol. 9, no. 1, pp. 97–104. https://doi.org/10.12962/j25481479.v9i1.19848
20. Ali A.H. Computational method for unsteady motion of two-dimensional airfoil. *Journal of Engineering*, 2008, vol. 14, no. 4, pp. 1–17. https://doi.org/10.31026/j.eng.2008.04.21
21. Ali A.H. Aerodynamic characteristics of a rectangular wing using non-linear vortex ring method. *Journal of Engineering*, 2017, vol. 23, no. 4, pp. 1–17. https://doi.org/10.31026/j.eng.2017.04.08
22. Selig M.S., Lyon C.A., Giguère P., Ninham C.N., Guglielmo J.J. *Summary of Low-Speed Airfoil Data*, V. 2. Virginia Beach, Virginia, SoarTech Publications, 1996.
23. Menter F.R. Two-equation eddy-viscosity turbulence models for engineering applications. *AIAA Journal*, 1994, vol. 32, no. 8, pp. 1598–1605. https://doi.org/10.2514/3.12149
24. Menter F.R., Langtry R.B., Likki S.R., Suzen Y.B., Huang P.G., Völker S. A correlation-based transition model using local variables. *Proc. of the ASME Turbo Expo*, 2004, pp. 1–11.
25. Versteeg H.K., Malalasekera W. *An Introduction to Computational Fluid Dynamics: The Finite Volume Method*. Pearson Education, 2007, 520 p.

19. Parluhutan Y.M., Fahrudin F., Rhakasywi D. Investigating the impact of plain flap as lift enhancement on symmetrical airfoils // International Journal of Marine Engineering Innovation and Research. 2024. V. 9. N 1. P. 97–104. https://doi.org/10.12962/j25481479.v9i1.19848
20. Ali A.H. Computational method for unsteady motion of two-dimensional airfoil // Journal of Engineering. 2008. V. 14. N 4. P. 1–17. https://doi.org/10.31026/j.eng.2008.04.21
21. Ali A.H. Aerodynamic characteristics of a rectangular wing using non-linear vortex ring method // Journal of Engineering. 2017. V. 23. N 4. P. 1–17. https://doi.org/10.31026/j.eng.2017.04.08
22. Selig M.S., Lyon C.A., Giguère P., Ninham C.N., Guglielmo J.J. Summary of Low-Speed Airfoil Data, V. 2. Virginia Beach, Virginia: SoarTech Publications, 1996.
23. Menter F.R. Two-equation eddy-viscosity turbulence models for engineering applications // AIAA Journal. 1994. V. 32. N 8. P. 1598–1605. https://doi.org/10.2514/3.12149
24. Menter F.R., Langtry R.B., Likki S.R., Suzen Y.B., Huang P.G., Völker S. A correlation-based transition model using local variables // Proc. of the ASME Turbo Expo. 2004. P. 1–11.
25. Versteeg H.K., Malalasekera W. An Introduction to Computational Fluid Dynamics: The Finite Volume Method. Pearson Education, 2007. 520 p.

Authors

Ahmed Tawfeeq Mustafa Ali Abed — Magister, Lecturer Assistant, Aeronautical Engineering Department, College of Engineering, University of Baghdad, Baghdad, 10071, Iraq, SC 59392733600, https://orcid.org/0000-0002-8025-9367, a.t.abed@coeng.uobaghdad.edu.iq
Azad A. Hussein — PhD, Lecturer, Aeronautical Engineering Department, College of Engineering, University of Baghdad, Baghdad, 10071, Iraq, SC 57297985700, https://orcid.org/0000-0001-9792-7774, azad.a@coeng.uobaghdad.edu.iq
Saba Hafedh Mahdi — Magister, Lecturer Assistant, Aeronautical Engineering Department, College of Engineering, University of Baghdad, Baghdad, 10071, Iraq, https://orcid.org/0009-0009-9479-0536, saba.hafedh@coeng.uobaghdad.edu.iq

Авторы

Али Ахмед Тауфик Мустафа Абед — магистр, помощник преподавателя, Отделение авиационной техники Инженерного колледжа, Багдадский университет, Багдад, 10071, Ирак, SC 59392733600, https://orcid.org/0000-0002-8025-9367, a.t.abed@coeng.uobaghdad.edu.iq
А. Азад Хусейн — PhD, преподаватель, Отделение авиационной техники Инженерного колледжа, Багдадский университет, Багдад, 10071, Ирак, SC 57297985700, https://orcid.org/0000-0001-9792-7774, azad.a@coeng.uobaghdad.edu.iq
Хафед Саба Махди — магистр, помощник преподавателя, Отделение авиационной техники Инженерного колледжа, Багдадский университет, Багдад, 10071, Ирак, https://orcid.org/0009-0009-9479-0536, saba.hafedh@coeng.uobaghdad.edu.iq

Received 04.05.2025
Approved after reviewing 10.10.2025
Accepted 12.11.2025

Статья поступила в редакцию 04.05.2025
Одобрена после рецензирования 10.10.2025
Принята к печати 12.11.2025